Electrochimica Acta 484 (2024) 144039

Contents lists available at ScienceDirect

Electrochimica Acta

journal homepage: www.journals.elsevier.com/electrochimica-acta

Evidence of transient potentials in ion-selective electrodes based on thin-layer ion-exchange membranes

Andres F. Molina-Osorio [a], Gastón A. Crespo [a,b], María Cuartero [a,b,*]

[a] Department of Chemistry, School of Engineering Science in Chemistry, Biochemistry and Health, KTH Royal Institute of Technology, Stockholm SE-100 44, Sweden
[b] UCAM-SENS, Universidad Católica San Antonio de Murcia, UCAM HiTech, Avda. Andres Hernandez Ros 1, Murcia 30107, Spain

ARTICLE INFO

Keywords:
Permselective membranes
Voltammetric ion-selective electrodes
Charge transfer
Transient potential
Membrane interfaces

ABSTRACT

Polymeric membranes with ion-exchange properties have found numerous applications in water treatment, dialysis, energy storage, chemical sensors, and bio-interfaces, among others. Notably, it is common to operate under non-equilibrium conditions while pursuing specific features (e.g., current generation) through an electron-to-ion mechanism. To maximize the final performance, it is crucial to understand the role of each interface within the system, which becomes complex when the device is tailored with several materials and films. This is the case for ion sensors based on thin membranes in backside contact with a redox active conducting polymer. Herein, we investigate such a system operating under a charge transfer mechanism, which features electroneutrality maintenance as the main driving force upon application of a linear sweep potential. This potential is modeled as being unequally distributed among the various system interfaces. Our results demonstrate and quantify the existence of a transient membrane potential at the membrane-electrolyte interface, owing to the implementation of a strategical measurement point on the buried membrane side and connected to a built-in electrometer for the exclusive acquisition of the potential difference at such an interface. The transient membrane potential was found to be <1 % of the total applied potential, meaning that the ion-transfer process at the electrolyte-membrane interface is less energetically costly that the electron transfer and doping processes occurring at the conducting polymer side. This small contribution can be potentiated by increasing the ion-exchange capacity of the membrane, which indirectly enlarges the system current and serves as a strategy for increasing the efficiency of the device.

1. Introduction

Liquid polymeric membranes doped with ionic sites are used in multiple technological approaches, such as water treatment [1], dialysis procedures [2], energy storage [3,4], bio-interfaces [5], and sensors [6]. These membranes act mainly as separation phases providing the partition or ion transfer/exchange when in contact with a second phase, usually another liquid or a gas. For instance, when a doped membrane is adjacent to an electrolyte solution, an electrostatic equilibrium is generated in the form of two parallel layers of charge at the corresponding interface (i.e., the electrical double layer, EDL), which, in turn, manifests as a potential at the interface [7]. This phenomenon has been widely exploited in potentiometric ion-selective electrodes (sensors) based on membranes of 200–300 μm in thickness, demonstrating a Nernstian relationship between the membrane potential (or the so-called phase boundary potential) and the concentration of ions in each phase [8].

Considerable efforts have been devoted to the understanding of this electrostatic equilibrium at the molecular level as well as the physicochemical properties of the EDLs at membrane/electrolyte interfaces [9]. In contrast to equilibrium conditions, little is known about the dynamic electrochemical properties of ionically doped membranes, which become even more complex whether they are constrained to nano-dimensions. Evidently, these properties become relevant when there is an external polarization driving ion transfer reactions between the membrane and the electrolyte [10]. Such is the case in biological plasma membranes (5–10 nm in thickness), where the concentrations of sodium and potassium significantly differ on both sides, thus creating a transmembrane potential that serves as the driving force for ion transport (e.g., the sodium–potassium pump) [11]. Fundamentally speaking,

* Corresponding author at: Department of Chemistry, School of Engineering Science in Chemistry, Biochemistry and Health, KTH Royal Institute of Technology, Stockholm SE-100 44, Sweden; UCAM-SENS, Universidad Católica San Antonio de Murcia, UCAM HiTech, Avda. Andres Hernandez Ros 1, Murcia 30107, Spain.
E-mail address: mariacb@kth.se (M. Cuartero).

https://doi.org/10.1016/j.electacta.2024.144039
Received 22 November 2023; Received in revised form 8 February 2024; Accepted 29 February 2024
Available online 1 March 2024

external polarization pushes the membrane away from its equilibrium to a transition state; thereafter, spontaneous relaxation depends on how the ionic charge is reorganized within the membrane and more importantly, at the membrane/electrolyte interface(s).

The EDL formation is also relevant in the electrochemical responses of certain systems where heterogeneous charge transfer occurs [12,13]. As a result, the metal electrode/electrolyte interface has been extensively investigated regarding electrochemical processes that depend on the dynamics of ions. Although some aspects are still under discussion [14], it is generally accepted that a charge excess at the metal surface generates a polarization event through an electric field that penetrates the electrolyte phase [15]. The penetration depth, formally called the Debye length (λ_D), depends on the dielectric properties of the medium. For highly conductive electrolyte solutions, λ_D is on the order of 1–100 nm [16–18]. Globally, the polarization input causes the reorganization of ions near to the metal surface, where specific electrostatic interactions occur. Other systems interconnecting charge transfer and ion dynamics, such as the metal/ionic liquid [19] or liquid/liquid interfaces [20], are less understood. Nevertheless, it has been recognized that the EDL structure and the dynamics of the ions near the interface have key roles in the electrochemical responses of these systems [21].

Liquid polymeric membranes in connection to metallic electrodes modified with redox active species (e.g., conducting polymers, CP) present a widely interesting case of study. In essence, charge reorganization occurs at two levels: the buried membrane interface and the membrane-electrolyte interface [22,23]. This class of systems is currently widely encountered in solar cells, batteries, as well as sensors, being crucial in their overall performances [24]. However, while evidently necessary, it is challenging to understand the connection between the global charge-based mechanism and the electrochemical properties of the devices, due to the complexity in obtaining empirical observations at both membrane interfaces. Notably, the metallic electrode could be also modified with self-assembled monolayers or certain nanostructures [25,26], instead of the CP.

In this work, we investigate how to reach empirical observations of any potential created at the membrane-electrolyte interface under an external polarization input. We hypothesize that such a potential is directly linked with the entire perturbation of the system, and specifically with the ion dynamics and charge separation occurring in the liquid membrane. We propose an additional measurement point (referred to here as the sensor electrode, SE) from the buried side of the membrane to allow for the exclusive monitoring of the potential at the membrane-electrolyte interface. The reported observations will evidence the effective polarization of buried interfaces and at a more controlled level, be particularly relevant for ion sensors utilizing non-equilibrium conditions and photo-electrochemical devices containing multiple interfaces (e.g., solar cells, and batteries).

2. Experimental section

2.1. Reagents

All chemicals were used as received without any further purification. All aqueous solutions were prepared using deionized water (> 18 MΩ. cm). 3-octylthiophene (97 %, OT), lithium perchlorate (> 98 %, $LiClO_4$), high molecular weight poly(vinyl chloride) (PVC), bis(2-ethylhexyl) sebacate (DOS), sodium tetrakis[3,5-bis-(trifluoromethyl)phenyl] borate (NaTFPB), 4,4′-Dinonyl-2,2′-bipyridine (97 %), potassium hexachloroosmate (technical grade, K_2OsCl_6), ammonium hexafluorophosphate (> 95 %, NH_4PF_6), potassium chloride (99.5 %, KCl), tetrahydrofuran (> 99.9 %, THF) and acetonitrile (anhydrous, > 99.8 %) were purchased from Sigma Aldrich. The dinonyl bipyridyl Os(II)/Os(III) compound $[Os(II)(dnbpy)_3(PF_6)_2$ was prepared as reported elsewhere [27].

2.2. Synthesis of the poly (3-octylthiophene) film

The electropolymerization of the poly (3-octylthiophene) (POT) film was carried out on the glassy carbon (GC) disk of a Pt-GC ring-disk electrode (RDE, 5 mm disc of GC with a concentric Pt ring at a distance of 375 μm, Metrohm) using a 0.1 M solution of 3-octylthiophene and $LiClO_4$ in acetonitrile. The films were grown under galvanostatic conditions by applying a current density of 0.875 mA cm^{-2} for 20 s (**Fig. S1**). Then, the films were cycled from 0 to 1.25 V (10 scans) and discharged at 0.2 V for 360 s in a 0.1 M solution of $LiClO_4$ in acetonitrile. The films were afterwards rinsed with pure acetonitrile and THF, and dried under a nitrogen stream for 1 min.

2.3. Preparation of the membranes

The membrane cocktails were prepared by dissolving 1.87 mg of PVC, 3.75 mg of DOS and different amounts of NaTFPB in 500 μL of THF. 30 μL of the cocktail was spin coated onto the POT-based RRDE at 1500 rpm for 60 s, homogenesouly covering the entire surface. For membranes containing dinonyl bipyridyl Os(II)/Os(III) compound $[Os(II)(dnbpy)_3(PF_6)_2$, 30 μL of a cocktail containing 1.87 mg of PVC, 3.75 mg of DOS, 1.10 mg of NaTFPB and 0.64 mg of $Os(II)(dnbpy)_3$ was spin coated onto the bare Pt-GC RRDE at 1500 rpm for 60 s, homogeneously covering the entire surface with a membrane thickness of ca. 200 nm [28].

2.4. Description of the experimental setup

The experimental setup designed for the generation and measurement of $\Delta\phi_{tr}$ is presented in Fig. 1. It consists of the GC disk in the RDE acting as the working electrode, (WE) and the concentric Pt ring acting as the sensing electrode (SE). While only the WE was covered with POT, both the WE and SE were properly covered by the thin membrane. The RDE is immersed in the electrolyte solution containing the reference and counter electrodes (RE and CE respectively) for the electrochemical measurements. The SE was strategically suited and connected to a built-in electrometer dedicated to acquiring the potential difference at the

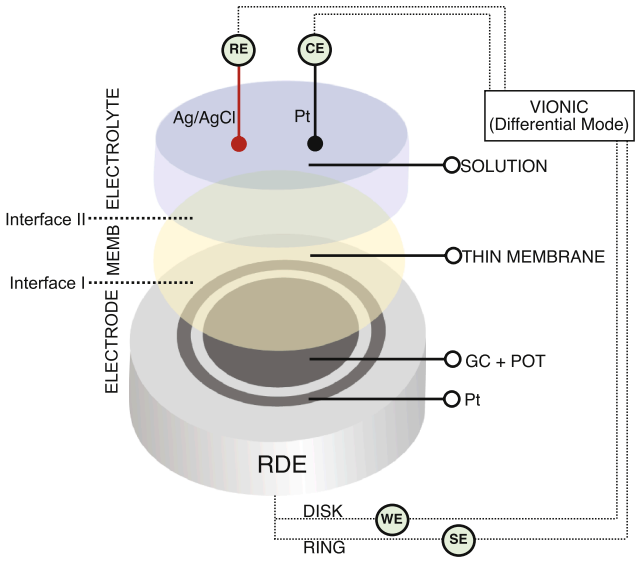

Fig. 1. Schematics of the experimental setup. The GC disk in the RDE modified with POT and with the doped thin membrane on top. The membrane entirely covered both the POT-GC disk and the Pt ring. The RDE is in contact with an aqueous solution of the electrolyte, in which the RE and CE are immersed. The disk in the RDE acts as the WE and the ring as the SE. All the electrodes are conveniently connected to the Vionic instrument operating under differential mode.

interface between the membrane and the electrolyte with respect to the RE (differential mode). Specifically, the measurements were performed in a Vionic potentiostat/galvanostat (Metrohm Nordic), using a single junction Ag/AgCl/3 M KCl as the RE and a Pt rod as the CE. The SE detects the equilibrium potential ($\Delta\phi_{eq}$) or the transient potential ($\Delta\phi_{tr}$) depending on whether the system is at equilibrium conditions or not. The input impedance of the electrometer is >1 TΩ; therefore, the effect of the ohmic drop on the membrane potential was minimized.

3. Results and discussion

3.1. The fundamental principle for the generation of the transient membrane potential

Liquid polymeric membranes doped with ionic sites can be utilized differently according to the final application of the device into which they are integrated. A membrane can be sandwiched between two electrolyte solutions, or between a modified metal electrode and an electrolyte solution. Considering the latter set-up, at equilibrium conditions, a potential difference is observed between the membrane and electrolyte phases due to the formation of an EDL. This equilibrium potential ($\Delta\phi_{eq}$) depends on the ionic concentration of each phase and is the basic of traditional potentiometric measurements at zero current condition, which is a well-established electrochemical technique. When the equilibrium state is disturbed by introducing a certain charge in the membrane through the electrode-membrane interface (i.e., a polarization), a physical reorganization of the ionic sites occurs, resulting in an additional potential difference in the membrane-sample interface, which is expected to be of a transient nature ($\Delta\phi_{tr}$). In other words, the induction of charge imbalance triggers a series of interconnected charge transfer processes at the different interfaces. This includes an ion transfer (IT) event between the membrane and the electrolyte phases to preserve the overall electroneutrality, with the concomitant generation of a net current flowing through the system. Importantly, the described charge distribution and current generation may occur under a thin-layer regime in membranes with very low thicknesses (ca. 230 nm) [23,28]. As a result, no mass transport limitation in the film nor the solution (considering a sufficient electrolyte concentration, ~mM) applies. In this work, we aim to provide empirical observations and an appropriate description of $\Delta\phi_{tr}$ in doped thin membranes under polarization conditions.

At the equilibrium, a potential is established at the membrane-electrolyte interface (in Fig. 1: Interface II, $\Delta\phi_{eq}$). This potential is related to the ion concentrations (strictly activities) in the membrane and the electrolyte solution through the well-known Nernst equation [29]:

$$\Delta\phi_{eq} = \Delta\phi_I^0 + \frac{RT}{z_I F} ln \frac{a_I^m}{a_I^{aq}} \quad (1)$$

where z_i is the charge, $\Delta\phi_I^0$ indicates the standard ion transfer potential, and a_I^m and a_I^{aq} represent the activity of ion I in the membrane and aqueous solution respectively. When an external polarization input in the form of an anodic linear sweep potential (E_{app}) is applied between the WE and RE, a current (j_{ET-IT}) flows between the WE and the CE. This current is associated with a series of coupled charge-transfer processes through the different interfaces, as illustrated in Fig. 2**a**. Notably, this figure has been conceived for two cases: (i) the redox element is incorporated on top of the electrode substrate (e.g., electropolymerized POT), and (ii) the redox element is directly dissolved in the membrane (e.g., the Os(II)/Os(III) compound directly dissolved in the membrane). As such, the redox element is considered as a *Red/Ox* specie that changes its oxidation state because of an electron transfer (ET) process close to the electrode surface. Moreover, in the case of POT, it is known that its interface with the membrane is relatively fuzzy due to two reasons: (i) the insertion of the membrane into the lattice pores and (ii) the

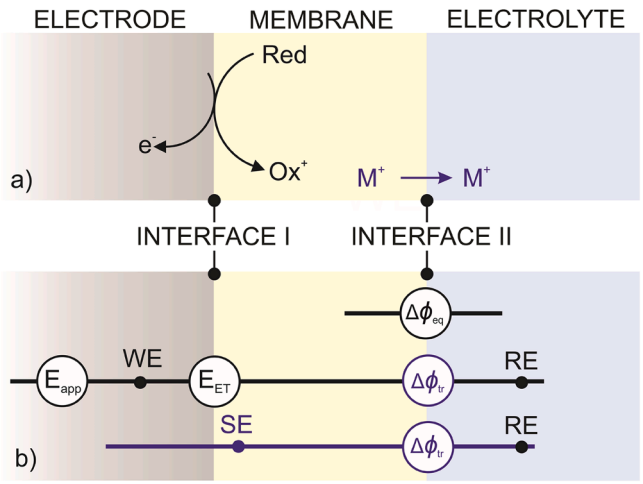

Fig. 2. **(a)** Mechanism of the interconnected charge transfer processes occurring in the system upon external polarization. **(b)** Correspondence between elements and potentials with respect to the total applied potential. Positioning of the WE, RE and SE to be able to measure $\Delta\phi_{tr}$.

expansion/relaxation of the polymer when oxidized/reduced, which occurs in a lower extent than in the bulk solution due to the confinement of the polymer between the electrode and the membrane [30–33].

Disturbing the equilibrium state by an applied potential, the basal state of the POT (reduced form, *Red*) is gradually oxidized to Ox^+ via an ET event. The created positive charge is compensated by the POT doping with the anionic part of the cation exchanger in the membrane ($TFPB^-$). Driven by electroneutrality maintenance, the ET event ultimately results in the expelling of the cationic counterpart of the cation-exchanger from the membrane to the solution: the IT event. Notably, in this work, the cation that is exchanged at the membrane-electrolyte interface is K^+. As demonstrated elsewhere, although the membrane initially contains Na^+TFPB^-, when immersed in millimolar KCl electrolyte, the total and fast replacement of Na^+ with K^+ occurs in the thin membrane; thus, the IT is ascribed to K^+ [23].

Assuming that the Ox^+ stabilization with $TFPB^-$ is not the rate-limiting step of the overall ET–IT process (actually, the ET-based doping event is known to be sufficiently fast and therefore, it can be neglected due to an absence of mass-transport dependence in the thin-layer membrane) [34], Eqs. (2) and 3 define the ET and IT processes at Interface I and Interface II, respectively:

$$Red_{(m)} \overset{k_{ET}}{\rightarrow} Ox^+_{(m)} + e^- \quad (2)$$

$$K^+_{(m)} \overset{k_{IT}}{\rightarrow} + K^+_{(aq)} \quad (3)$$

where the subscripts *m* and *aq* denote the membrane and the aqueous phase, and k_{ET} and k_{IT} are the potential-dependent kinetic constants for the ET and IT steps, respectively.

The kinetics of both steps (ET and IT) can be described by the dependence of k_{ET} and k_{IT} on the potential associated with ET and IT (E_{ET} and E_{IT}) [35]. The main challenge is indeed the rationalization of such potentials. A relationship among all the potential drops in the system can been formulated considering the total external polarization potential (E_{app}) [36]:

$$E_{app} = E_{ET} + E_{IT} + iR \quad (4)$$

with the *iR* term accounting for the ohmic drop between the WE and RE. Notably, the ohmic drop has been established as neglectable in systems

based on very thin membranes, such as those herein explored [28,36]. Although this relationship has been widely accepted by the electrochemistry community, to the best of our knowledge, there is a lack of empirical evidence confirming such a behavior. Therefore, we propose to address this missing piece of important knowledge with the designed SE, which is expected to provide experimental detection of the E_{IT} in the form of $\Delta\phi_{tr}$ and in relation to the polarization input (Fig. 2**b**). Effectively, the system is tailored to ensure that the *Red* (POT or indeed any other redox mediator) is excessive with respect to the cation-exchanger in the membrane; hence, $\Delta\phi_{tr}$ is expected to be limited by the concentration of $Na^{+}TFPB^{-}$ in the thin-layer membrane. This condition was selected to allow for the investigation of the effect of a more drastic charge unbalance in the system (i.e., an increase in the $Na^{+}TFPB^{-}$ generates an increase in the amount of POT^{+} that can be achieved in the polarization) in the $\Delta\phi_{tr}$.

3.2. Measurements of the transient membrane potential with the SE

Fig. 3**a** shows the cyclic voltammograms (WE readouts) of the system under study in 0.01 M KCl electrolyte and using a membrane containing 80 mmol kg^{-1} of NaTFPB (scan rate of 100 mV s^{-1}). A reversible Gaussian-shaped wave appears at 360 mV, being rather well-maintained in subsequent scans: the charge in the anodic peak is 113±6 μC cm^{-2}, the charge in the cathodic peak is 87.1 ± 5 μC cm^{-2}, $w_{1/2}$ is 1.1 for the cathodic and anodic peaks, and $|E_{peak,c} - E_{peak,a}|$ is 42 mV. These features suggested that the overall ET–IT process responsible for the voltametric wave (Eqs. (2) and 3) is not limited by diffusion in the solution phase, but it is mostly affected by other events occurring at the buried interface, since the diffusion within the membrane is expected to be fast [37].

To confirm that the SE redout unequivocally corresponded to the $\Delta\phi_{tr}$, we collected E_{app}, $\Delta\phi_{tr}$, and the current (j_{ET-IT}) as functions of the experimental time (from the E_{app}), Fig. 3**b**. The dynamic $\Delta\phi_{tr}$ displayed two peaks that coincided in time (and thus in E_{app}) with the voltammetric waves. Moreover, this behavior is totally reproducible in subsequent scans, confirming the reversibility of all the processes present in the system. The magnitude of $\Delta\phi_{tr}$ is 3.6 mV at the peak maximum, coinciding with an applied potential equal to the position of the anodic peak. Thus, $\Delta\phi_{tr}$ was the 0.64 % of the applied potential at that point. Considering Eq. (4), this result suggested that most of the applied potential is utilized for the ET (Interface I) rather than the IT (Interface II). Then, when the redox mediator (POT layer) was omitted in the system, the cyclic voltammetric response displays no peaks, coinciding with the absence of peaks in the potential signal recorded by the SE (Fig. 3**c**). Accordingly, no IT occurs at the Interface II and only a double layer capacitive process is observed.

The ET–IT mechanism only involves the spatial domain coinciding with the diameter of the GC disk in the RDE, which is supported by the thin-layer regime in the membrane (i.e., no diffusion contribution). Importantly, the Pt ring (the SE) is positioned 325 μm far from the ET–IT area (the WE, GD disk) but still in contact with the membrane. This means that any charge rearrangement in the system will not affect the output (rest) voltage of the Pt, but only a change will manifest when the interfacial (membrane-electrolyte) potential varies. Effectively, the distance between the disk and the risk is ca. 1600 times larger than the membrane thickness (325 μm versus 200 nm), implying that the lower diffusion time along the membrane thickness dictates the prevalence of longitudinal charge transfer instead of transversal. An estimation of the diffusion time of an ion with a diffusion coefficient of 10^{-7} cm^2 s^{-1} in the membrane and considering the Stokes-Einstein relation for 1D diffusion provided times of 4 ms versus 3 h for longitudinal (along the membrane thickness) and transversal (in the direction of the SE) charge movement.

The empirical finding regarding the magnitude of $\Delta\phi_{tr}$ (ca. 4 mV, see above) coincides with previous theoretical predictions stating that the potential associated with the IT should be on the order of 5 mV [23]. Accordingly, the voltammetric peak is mainly dominated by the E_{ET} rather than E_{IT}. Indeed, in Mao et al.'s paper, it was calculated that the ET in POT involves a much broader potential wave than that associated with the IT [38]. Also, the authors stated that a higher ion-exchanger concentration in the membrane will produce an ET wave closer to the IT wave. It is our understanding that this latter prediction indicates that an increase in the $Na^{+}TFPB^{-}$ present in the membrane will translate into a higher E_{IT}, given that the E_{ET} is well maintained. As far as we know, at the time of writing, our results are the very first empirical evidence of the presence and magnitude of the membrane potential, beyond already published semi-empirical predictions [23,38].

3.3. Effect of the membrane's ionic concentration on the transient membrane potential

The effect of the membrane ionic concentration on the $\Delta\phi_{tr}$ was explored by varying the concentration of NaTFPB in the membrane from 0 to 160 mmol kg^{-1}. In principle, it is expected that, the more $TFPB^{-}$ in the membrane, the greater the POT^{+} charge that can be generated due to the polarization input. Therefore, the total exchange capacity of the membrane should increase, as should the charge under the voltammetric peak. Fig. 4**a** shows how the voltammetric peak (both current and charge) increases with the NaTFPB concentration in the membrane. Then, in the absence of NaTFPB, only a capacitive current was observed. In all the cases, the corresponding control experiment without the redox mediator (POT) confirmed the need for its presence to generate the charge transfer mechanism (**Figs. S2–S4**, *Supporting Information*). Furthermore, excellent reproducibility is displayed (**Table S1**, *Supporting Information*).

With respect to the charge under the peak, analyzing only the anodic part as an example, these yield values of 54.1 ± 5.5, 113 ± 6.0 and 234 ± 5.5 μC cm^{-2} for NaTFPB concentrations of 40, 80, and 160 mmol kg^{-1}, respectively. Hence, as expected, the charge was found to increase with the NaTFPB concentration. Considering that the POT charge deposited

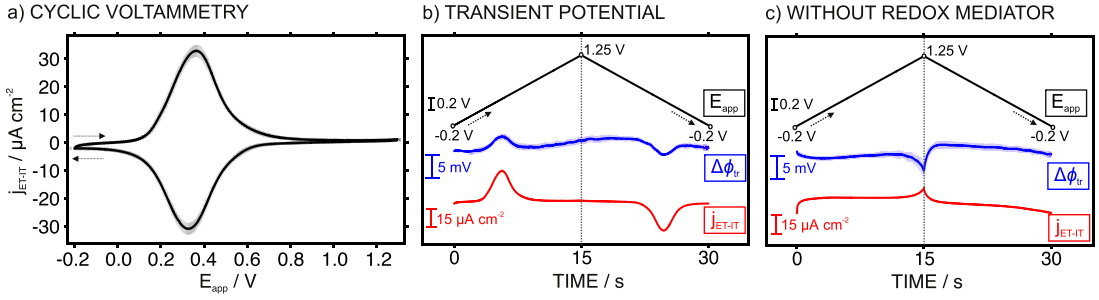

Fig. 3. (a) Cyclic voltammogram using a membrane with 80 mmol kg^{-1} of NaTFPB. **(b)** Corresponding temporal traces for the E_{app}, $\Delta\phi_{tr}$ (SE) and the recorded current (j_{ET-IT}). **(c)** Control experiment without the presence of the redox mediator (POT). The displayed data is the average of three measurements (standard deviations are provided as shaded regions). Arrows indicate the direction of the applied potential. The dotted line indicates the potential direction switch in the voltammetric experiment. Electrode= POT-membrane. Electrolyte=0.01 M KCl. Scan rate=100 mV s^{-1}.

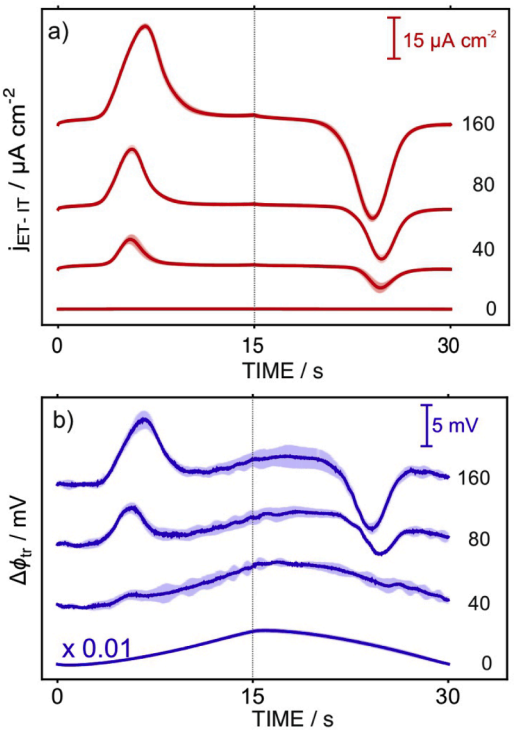

Fig. 4. Temporal traces of **(a)** the current density (j_{ET-IT}) and **(b)** the transient membrane potential ($\Delta\phi_{tr}$) using membranes with increasing NaTFPB concentrations. All the data are averages of three measurements (standard deviations are provided in shaded regions). The dotted line indicates the potential direction switch in the voltammetric experiment. Electrode= POT-membrane. Electrolyte=0.01 M KCl. Scan rate=100 mV s^{-1}.

in the GC disk is estimated to be 17.5 mC cm^{-2} (according to the results from the galvanostatic synthesis, **Fig. S1**), the percentages of usage of the total available POT charge are calculated as 0.31, 0.64, and 1.33 % for 40, 80, and 160 mmol kg^{-1} of NaTFPB, respectively. Fig. 4**b** depicts the temporal profiles of the $\Delta\phi_{tr}$ recorded by the SE. In the absence of NaTFPB, no peaks appeared, in total agreement with the absence of voltammetric peaks. Then, as the NaTFPB in the membrane increases, $\Delta\phi_{tr}$ manifested in the form of increasing peaks. For each membrane composition, the maximum change in $\Delta\phi_{tr}$ well corresponded to the peak potential in the voltammetry redout. The $\Delta\phi_{tr}$ values were 0.6, 3.6, and 6.3 mV at the peaks found for 40, 80, and 160 mmol kg^{-1} of NaTFPB. It can be concluded that as the maximum $\Delta\phi_{tr}$ value increases with the NaTFPB concentration, constituting 0.1, 0.64, and 0.96 % of the applied potential at that point when using 40, 80, and 160 mmol kg^{-1} of NaTFPB. Thus, the IT weight in relation to the external polarization increases.

Importantly, the behavior of the membranes with no ionic sites (i.e., [NaTFPB] = 0 mmol kg^{-1}) was further explored. In the absence of the redox mediator (**Fig. S5**, *Supporting Information*), $\Delta\phi_{tr}$ linearly increased until a total change of 125 mV, and then returned to its initial value in the reverse voltammetric scan. The total change was approximately 25 times higher than that found for the membrane with 40 mmol kg^{-1} NaTFPB (**Fig. S5a**). On the other hand, in the presence of the redox mediator (**Fig. S5b**), $\Delta\phi_{tr}$ for a membrane with no NaTFPB linearly increased until a total change of 340 mV, and then returned to its initial value in the reverse voltammetric scan. In this case, the maximum change in $\Delta\phi_{tr}$ was ca. 70 times higher than that obtained for a membrane with 40 mmol kg^{-1} NaTFPB. Accordingly, the effect of the presence and increase in NaTFPB on $\Delta\phi_{tr}$ showed the transition of the membrane from a dielectric to an ionic conductive material [39]. Thus, when the membrane behaves as a dielectric material ([NaTFPB] = 0 mmol.kg^{-1}), a large potential drop is observed within the membrane, being the potential drop at Interface I is not sufficient to oxidize the redox mediator. On the contrary, when the membrane is ionic conductive ([NaTFPB] $\geq$ 40 mmol kg^{-1}), the potential drop across the membrane significantly decreases and is indeed confined to the Interface I, where the redox mediator is oxidized.

Overall, it can be concluded that regardless of the composition of the membrane and in presence of the redox mediator, the largest potential drop in the system always occurs at the Interface I in relation to the ET event. Indeed, the distribution of the potential drop is mostly affected by the concentration of NaTFPB. Moreover, in agreement with EDL relaxation theories, the external polarization sems to decay rapidly from Interface I over a distance that strongly depends on the ionic concentration of the membrane [40,41]. In the absence of ionic sites, the external polarization decays over a longer distance from the WE; hence, 24 % of the total potential drop occurs within the membrane phase. When the ionic concentration in the membrane increases, the external polarization decays more rapidly along the very few nanometers from the modified electrode surface; thus, the potential drop in the membrane represents less than 1 % of the external polarization. Interestingly, the effect of the ionic site concentration in the membrane can be considered an analogous to the effect of the supporting electrolyte concentration (always at relatively high concentrations to minimize diffusion effects) in the case of bulk aqueous solutions, where the higher the concentration is, the narrower the EDL thickness and the stronger the electric field near the electrode surface [18,42,43]. This finding shed light on how to enlarge the system current and the efficiency of any device similarly based on a multimaterial-layering design providing interconnected charge-transfer-event response mechanism. The selection of the conducting polymer will dictate the potential distribution along the system interfaces, whereas the ion-exchange capacity is responsible for the magnitude of the current output.

3.4. *Interpretation of the physicochemical contributions to the global magnitude of the transient membrane potential*

The experiment in the absence of POT is indeed a background-related potential that follows the external polarization. If such a potential is subtracted to the profiles displayed by the POT-membrane systems (Fig. 4**b**), the results will provide the pure $\Delta\phi_{tr}$ in the form of a close-to-Gaussian peak. On one hand, the background contribution is present in the experiments carried out with and without POT: the corresponding potential may be associated with the bulk ionic resistance in the membrane and therefore, it is labeled here as the *ionic potential drop*. On the other hand, the peak is only observed in the presence of both POT and cationic sites, and this agrees with the corresponding current waves in the voltammetric response. Accordingly, the peak can be ascribed to a positive charge excess injected at the buried membrane interface, originating from the oxidation of the POT film. This excess creates a potential difference at the membrane-electrolyte interface that is the driving force for the IT step, labeled here as the *charge injection potential.*

The concept is exemplified in Fig. 5**a,** considering the anodic part of the $\Delta\phi_{tr}$ trace observed for the membrane containing 160 mmol kg^{-1} of NaTFPB. The ionic potential drop (experiment in the absence of POT, *solid black line*) is subtracted from the $\Delta\phi_{tr}$ trace (*solid blue line*) to obtain the pure charge injection potential (*dashed blue line*). Moreover, this latter potential correlates with the accumulative dynamic charge observed under the voltammetric experiment, as depicted in Fig. 5**b**. In essence, the time window for the peak shown in $\Delta\phi_{tr}$ and in the sigmoidal-based change of the charge rather coincide. Also, the inflection point timing of the latter agrees with the timing for the maximum $\Delta\phi_{tr}$ (ca. 6.5 s).

The physicochemical meanings of the ionic potential drop and the charge injection potential can be investigated from the dependence of $\Delta\phi_{tr}$ on the concentration of the ionic sites (i.e., NaTFPB) in the membrane. A significant decrease in the magnitude of the ionic potential drop was observed when the concentration of the ionic sites is increased from 0 to 160 mmol kg^{-1} (**Fig. S4**). Considering the inverse relationship

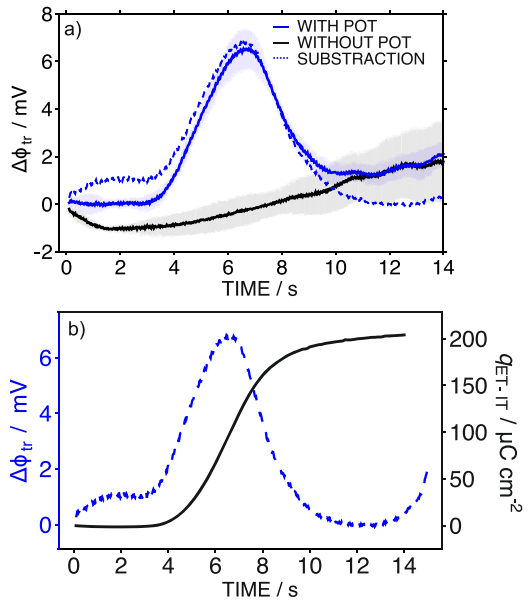

Fig. 5. (a) Subtraction of the ionic potential drop from the anodic $\Delta\phi_{tr}$ trace of the membrane containing 160 mmol kg^{-1} of NaTFPB to obtain the charge injection potential. (b) Correspondence of the charge injection potential and the accumulative dynamic charge observed under the voltammetric experiment. Electrode= POT-membrane. Electrolyte = 0.01 M KCl. Scan rate=100 mV s^{-1}.

that commonly exists between the ionic concentration and the resistance of the membrane [44,45], the ionic potential drop is likely associated with the membrane resistance. Then, in the case of the charge injection potential, the observed behavior is completely distinct: the higher the concentration of the ionic sites in the membrane, the higher the charge injection potential and consequently, the higher peak current in the voltammogram.

The charge injection potential is evidently a consequence of a redox-mediated polarization process, where a redox reaction in connection to the membrane –it could be at the buried membrane interface or within the membrane element, as in the case of the osmium compound presented in the next section– injects a charge excess that changes the potential of the entire membrane phase and ultimately polarizes the membrane-electrolyte interface. Notably, the mechanism for a redox-mediated polarization bears a resemblance to the traditional polarization of a metal-electrolyte interface. In the latter situation, the interface with the electrolyte is polarized by injecting electrons into the metal and raising its Fermi level [35], whereas in the former, polarization occurs via the injection of a charge excess and a change in the electrochemical potential of the ions in the membrane.

The relationship between charge injection and charge carrier dynamics in doped thin membranes and semiconductors also share some similarities. Despite the charge carriers in these materials presenting different nature (ions in membranes, and electron-hole pairs in semiconductors), the rate of charge injection is greatly influenced by the mobility of these carriers [46,47]. This fact has already been demonstrated in p-type semiconductors, where a direct proportionality exists between the concentration of hole transport agents, hole mobility, and charge injection. In doped thin membranes, the results presented in this work has revealed that the role of an ionic site in the membrane is analogous to that of a hole transport in a semiconductor.

3.5. The case of the redox mediator dissolved directly in the membrane

The case where the redox mediator is directly dissolved in the membrane was also investigated. The POT film was replaced by the lipophilic dinonyl bipyridyl Os(II)/Os(III) compound [Os(II)(dnbpy)$_3$(PF$_6$)$_2$] at a concentration of 75 mmol kg^{-1} and accompanied with 200 mmol kg^{-1} of NaTFPB. Notably, in contrast to the case of POT, an excess of NaTFPB allows for the visualization of cation transfer instead of anion transfer, since in this case, the direct entrance of anions from the solution to stabilize the oxidized Os^{3+} is possible. The compound is synthetized as described elsewhere [27]. Fig. 6**a** shows the cyclic voltammograms (WE readout) of this system in 0.01 M KCl electrolyte (scan rate of 100 mV s^{-1}). A voltammetric wave appeared at 850 mV and was rather well-maintained in subsequent scans: the charge of the anodic peak was 106±4 μC cm^{-2}, the charge of the cathodic peak was 58±5 μC cm^{-2}, and $|E_{peak,c} - E_{peak,a}|$ was 63 mV. In this case, the ET–IT charge transfer reaction follows a mechanism in which the oxidation of Os moieties in the membrane occurs from Os^{2+} to Os^{3+}, which is accompanied by an IT event at the membrane-electrolyte interface to keep electroneutrality, as previously demonstrated [27].

We can identify three main differences between the voltammograms displayed by electrodes prepared with the POT film or the $Os^{2+/3+}$ compound. The first difference involves the reversibility of the charge transfer process. With POT as the mediator, the potential difference between the voltammetric anodic and potential waves ($|E_{peak,c} - E_{peak,a}|$) is 42 mV, and the peak charge ratio is 1.1. However, with the $Os^{2+/3+}$ compound, $|E_{peak,c} - E_{peak,a}|$ increases to 63 mV and the peak charge ratio decreases to 0.6. These values suggest a higher reversibility of the ET–IT process in the presence of POT. The second difference is found in the half wave-potential ($E_{1/2}$). With POT, a value of $E_{1/2}$ = 340 mV is obtained, whereas, with $Os^{2+/3+}$, this value increases up to 800 mV. In principle, the shift in $E_{1/2}$ is likely related to a change in the standard ET potential of $Os^{2+/3+}$ with respect to that of POT [27]. The last difference is observed in the shape of the voltammetric peak, where a tail in the final part may indicate that, with $Os^{2+/3+}$ diffusion effects become significant at the experimental scan rate, in contrast to the POT immobilized/confined at the electrode surface.

Fig. 6**b** depicts the E_{app}, $\Delta\phi_{tr}$, and j_{ET-IT} as functions of the experimental time in the electrodes prepared with the $Os^{2+/3+}$ in the

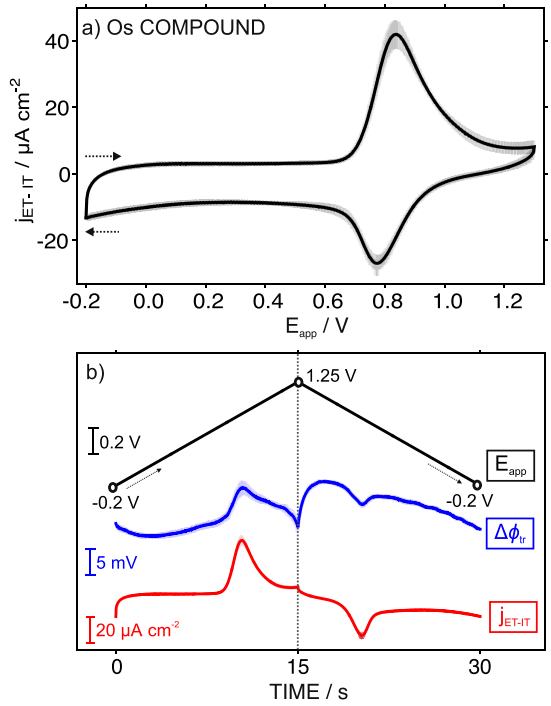

Fig. 6. (a) Cyclic voltammetry using a membrane with 200 mmol kg^{-1} of NaTFPB and 75 mmol kg^{-1} of dinonyl bipyridyl Os(II)/Os(III). **(b)** Corresponding temporal traces for E_{app}, $\Delta\phi_{tr}$ (SE), and the recorded current (j_{ET-IT}). All the data are the averages of three measurements (standard deviations are provided as shaded regions). The dotted line indicates the potential direction switch in the voltammetric experiment.

membrane. The $\Delta\phi_{tr}$ presented an analogous trace to that observed for POT: two peaks in $\Delta\phi_{tr}$ that coincide in time (and thus in E_{app}) with the anodic and cathodic voltammetric peaks. However, with a lower reversibility: the value for $\Delta\phi_{tr}$ at the peak is higher in the anodic scan than in the cathodic scan (6.5 versus 2.5 mV). In the anodic scan, $\Delta\phi_{tr}$ constituted 0.63 % of the applied potential at that point, which is a very similar value to that observed for POT. Overall, the shape for $\Delta\phi_{tr}$ is slightly distorted compared to that for POT. Furthermore, there is a delay in the peak to appear, which is related to the change in the standard ET potential of the redox probe (i.e., 10.4 s for $Os^{2+/3+}$and 6.5 s for POT in the $\Delta\phi_{tr}$ peaks, and standard ETs of 0.95 V and 0.70 V, for POT and $Os^{2+/3+}$, see **Fig. S1c** and [27]). Advantageously, the experiments demonstrated the validity and versatility of the developed methodology to observe and interpret $\Delta\phi_{tr}$ in systems based on different kinds of redox mediators.

4. Conclusions

The transient potential across thin polymeric membranes operating under external polarization has been monitored, quantified, and interpreted. Two systems have been investigated, differing in the way in which the redox mediator is implemented in connection to the membrane: (i) an electropolymerized redox active conducting polymer covered with a nanometer-sized membrane layer that contains a dopant lipophilic anion; and (ii) a nanometer-sized membrane containing a dissolved redox mediator capable of being doped with any lipophilic anion upon oxidation. The operation principles for both systems are governed by a coupled electron-transfer-ion-transfer mechanism (ET–IT), with electroneutrality maintenance as the main driving force upon application of a linear sweep potential. It was found that in cases where the ionic concentration in the membrane is very low or null, the membrane behaves as a pure dielectric material and more than 75 % of the applied potential decays within the membrane domain. When the ionic concentration increases, the transition of the membrane into a conductive phase was demonstrated, with the applied potential mostly confined to the buried membrane interface. Additionally, when the membrane is in contact with a redox mediator, the applied potential drives an ET reaction that injects a charge excess into the membrane. This excess polarizes the membrane-electrolyte interface by a value that varies between 0.6 and 6.3 mV, depending on the concentrations of ionic sites in the membrane. Such a small polarization is enough to drive rapid IT reactions involving the electrolyte, such as the transfer of K^+. Finally, this work demonstrates that the effective polarization of membrane-electrolyte interfaces is mainly dependent on two parameters: (i) the charge excess injected into one of the phases, and (ii) the concentrations of ionic sites (conductivity) in the membrane. By controlling these two parameters, polarization at the membrane-electrolyte interface can be maximized, and efficiency of charge separation can be conveniently improved, which is a key factor in certain devices including such interfaces, e.g., those used in water treatment, dialysis procedures, energy storage, physical/chemical sensors, and bio-interfaces, among others.

CRediT authorship contribution statement

Andres F. Molina-Osorio: Methodology, Software, Validation, Formal analysis, Investigation, Data curation, Writing – original draft, Visualization. **Gastón A. Crespo:** Conceptualization, Methodology, Validation, Formal analysis, Writing – original draft, Writing – review & editing, Supervision. **María Cuartero:** Conceptualization, Methodology, Formal analysis, Resources, Writing – original draft, Writing – review & editing, Visualization, Supervision, Project administration, Funding acquisition.

Declaration of competing interest

The authors declare the following financial interests/personal relationships which may be considered as potential competing interests: Maria Cuartero reports financial support was provided by European Research Council. Maria Cuartero reports financial support was provided by Swedish Research Council. If there are other authors, they declare that they have no known competing financial interests or personal relationships that could have appeared to influence the work reported in this paper.

Data availability

Data will be made available on request.

Acknowledgment

This project received funding from the European Research Council (ERC) under the European Union's Horizon 2020 Research and Innovation Programme (Grant Agreement No. 851957). MC acknowledges the Swedish Research Council (Project Grant VR-2019–04142). The authors thank Adam Tillo for the synthesis of the Os compound.

Supplementary materials

Supplementary material associated with this article can be found, in the online version, at doi:10.1016/j.electacta.2024.144039.

References

[1] D.M. Warsinger, S. Chakraborty, E.W. Tow, M.H. Plumlee, C. Bellona, S. Loutatidou, L. Karimi, A.M. Mikelonis, A. Achilli, A. Ghassemi, A review of polymeric membranes and processes for potable water reuse, Prog. Polym. Sci. 81 (2018) 209–237.
[2] P. Wang, M. Wang, F. Liu, S. Ding, X. Wang, G. Du, J. Liu, P. Apel, P. Kluth, C. Trautmann, Ultrafast ion sieving using nanoporous polymeric membranes, Nat. Commun. 9 (1) (2018) 1–9.
[3] X. Li, H. Zhang, Z. Mai, H. Zhang, Vankelecom, I. Ion exchange membranes for vanadium redox flow battery (VRB) Applications, Energy Environ. Sci. 4 (4) (2011) 1147–1160.
[4] A.U. Petersen, A.I. Hofmann, M. Fillols, M. Mansø, M. Jevric, Z. Wang, C.J. Sumby, C. Müller, K. Moth-Poulsen, Solar energy storage by molecular norbornadiene–quadricyclane photoswitches: polymer film devices, Adv. Sci. 6 (12) (2019) 1900367.
[5] Y.V. Lee, B. Tian, Learning from solar energy conversion: biointerfaces for artificial photosynthesis and biological modulation, Nano Lett. 19 (4) (2019) 2189–2197.
[6] R. Ishimatsu, A. Izadyar, B. Kabagambe, Y. Kim, J. Kim, S. Amemiya, Electrochemical mechanism of ion–ionophore recognition at plasticized polymer membrane/water interfaces, J. Am. Chem. Soc. 133 (40) (2011) 16300–16308.
[7] A. Moya, Theory of the formation of the electric double layer at the ion exchange membrane–solution interface, Phys. Chem. Chem. Phys. 17 (7) (2015) 5207–5218.
[8] E. Bakker, P. Bühlmann, E. Pretsch, The phase-boundary potential model, Talanta 63 (1) (2004) 3–20.
[9] L. Quoc Hung, Electrochemical properties of the interface between two immiscible electrolyte solutions: part i. equilibrium situation and galvani potential difference, J. Electroanal. Chem. Interfacial. Electrochem. 115 (2) (1980) 159–174.
[10] G.A. Crespo, E. Bakker, Dynamic electrochemistry with ionophore based ion-selective membranes, RSC. Adv. 3 (48) (2013) 25461–25474.
[11] A.A. Gurtovenko, I. Vattulainen, Membrane potential and electrostatics of phospholipid bilayers with asymmetric transmembrane distribution of anionic lipids, J. Phys. Chem. B 112 (15) (2008) 4629–4634.
[12] K. Hernández-Burgos, Z.J. Barton, J. Rodríguez-López, Finding harmony between ions and electrons: new tools and concepts for emerging energy storage materials, Chem. Mater. 29 (21) (2017) 8918–8931.
[13] O.M. Magnussen, A. Groß, Toward an Atomic-Scale Understanding of Electrochemical Interface Structure and Dynamics, J. Am. Chem. Soc. 141 (12) (2019) 4777–4790.
[14] K. Ojha, K. Doblhoff-Dier, M.T. Koper, Double-layer structure of the Pt (111)–aqueous electrolyte interface, Proc. Nat. Acad. Sci. 119 (3) (2022) e2116016119.
[15] S.M. Lu, J.F. Chen, Y.Y. Peng, W. Ma, H. Ma, H.F. Wang, P. Hu, Y.T. Long, Understanding the dynamic potential distribution at the electrode interface by stochastic collision electrochemistry, J. Am. Chem. Soc. 143 (32) (2021) 12428–12432.
[16] G. Cevc, Membrane Electrostatics, Biochimica et Biophysica Acta (BBA)-Reviews on Biomembranes 1031 (3) (1990) 311–382.
[17] A.M. Smith, A.A. Lee, S. Perkin, The electrostatic screening length in concentrated electrolytes increases with concentration, J. Phys. Chem. Lett. 7 (12) (2016) 2157–2163.
[18] M.Z. Bazant, K. Thornton, A. Ajdari, Diffuse-Charge Dynamics in Electrochemical Systems, Physical review E 70 (2) (2004) 021506.

[19] M. Belotti, X. Lyu, L. Xu, P. Halat, N. Darwish, D.S. Silvester, C. Goh, E. I. Izgorodina, M.L. Coote, S. Ciampi, Experimental evidence of long-lived electric fields of ionic liquid bilayers, J. Am. Chem. Soc. 143 (42) (2021) 17431–17440.
[20] G.C. Gschwend, A. Olaya, P. Peljo, H.H. Girault, Structure and reactivity of the polarised liquid–liquid interface: what we know and what we do not, Curr. Opin. Electrochem. 19 (2020) 137–143.
[21] I. Benjamin, Chemical Reactions And Solvation At Liquid Interfaces: A Microscopic Perspective, Chem. Rev. 96 (4) (1996) 1449–1476.
[22] Z. Zhang, X. Sui, P. Li, G. Xie, X.Y. Kong, K. Xiao, L. Gao, L. Wen, L. Jiang, Ultrathin and ion-selective Janus membranes for high-performance osmotic energy conversion, J. Am. Chem. Soc. 139 (26) (2017) 8905–8914.
[23] G.A. Crespo, M. Cuartero, E. Bakker, Thin layer ionophore-based membrane for multianalyte ion activity detection, Anal. Chem. 87 (15) (2015) 7729–7737.
[24] R. Joseph Kline, M.D. McGehee, M.F Toney, Highly oriented crystals at the buried interface in polythiophene thin-film transistors, Nat. Mater. 5 (3) (2006) 222–228.
[25] R. McNair, G. Szekely, R.A. Dryfe, Ion-exchange materials for membrane capacitive deionization, ACS. ES. T. Water. 1 (2) (2020) 217–239.
[26] Y. Yang, M. Cuartero, V.R. Gonçales, J.J. Gooding, E. Bakker, Light-addressable ion sensing for real-time monitoring of extracellular potassium, Angew. Chem. Int. Ed. 57 (51) (2018) 16801–16805.
[27] S. Jansod, L. Wang, M. Cuartero, E. Bakker, Electrochemical ion transfer mediated by a lipophilic Os(II)/Os(III) dinonyl bipyridyl probe incorporated in thin film membranes, Chem. Commun. 53 (78) (2017) 10757–10760.
[28] M. Cuartero, G.A. Crespo, E. Bakker, Polyurethane ionophore-based thin layer membranes for voltammetric ion activity sensing, Anal. Chem. 88 (11) (2016) 5649–5654.
[29] H.H. Girault, Electrochemistry at liquid-liquid interfaces, Electroanal Chem 23 (2010) 1–104.
[30] A.I. Kulapin, A.M. Mikhailova, E.G. Kulapina, Stabilizing potential of solid-contact sensors selective towards surface-active substances, Russ. J. Electrochem. 39 (2003) 585–590.
[31] J. Sutter, E. Lindner, R.E. Gyurcsányi, E. Pretsch, A polypyrrole-based solid-contact Pb2+-selective PVC-membrane electrode with a nanomolar detection limit, Anal. Bioanal. Chem. 380 (2004) 7–14.
[32] I. Robayo-Molina, G.A. Crespo, M. Cuartero, Usefulness of the distribution of relaxation time method in electroanalytical systems: the case of voltammetric ion-selective electrodes, ACS. Omega 9 (2024) 8162–8172.
[33] E. Jaworska, M. Mazur, K. Maksymiuk, A. Michalska, Fate of poly(3-octylthiophene) transducer in solid contact ion-selective electrodes, Anal. Chem. 90 (4) (2018) 2625–2630.
[34] Y. Liu, G.A. Crespo, M. Cuartero, Semi-empirical treatment of ionophore-assisted ion-transfers in ultrathin membranes coupled to a redox conducting polymer, Electrochim. Acta 388 (2021) 138634.
[35] A.J. Bard, L.R. Faulkner, Electrochemical Methods: Fundamentals and Applications, 2nd ed., Wiley, New York, 2001.
[36] Y. Kim, S. Amemiya, Stripping analysis of nanomolar perchlorate in drinking water with a voltammetric ion-selective electrode based on thin-layer liquid membrane, Anal. Chem. 80 (15) (2008) 6056–6065.
[37] A.F. Molina-Osorio, A. Wiorek, G. Hussain, M. Cuartero, G.A. Crespo, Modelling electrochemical modulation of ion release in thin-layer samples, J. Electroanal. Chem. 903 (2021) 115851.
[38] C. Mao, D. Yuan, L. Wang, E. Bakker, Separating boundary potential changes at thin solid contact ion transfer voltammetric membrane electrodes, J. Electroanal. Chem. 880 (2021) 114800.
[39] T. Dakin, Conduction and polarization mechanisms and trends in dielectric, IEEE Electrical Insul. Magaz. 22 (5) (2006) 11–28.
[40] S.W. Feldberg, Theory of relaxation of the diffuse double layer following coulostatic charge injection, J. Phys. Chem. 74 (1) (1970) 87–90.
[41] T.R. Brumleve, R.P. Buck, Numerical solution of the nernst-planck and poisson equation system with applications to membrane electrochemistry and solid state physics, J. Electroanal. Chem. Interfacial. Electrochem. 90 (1) (1978) 1–31.
[42] I. Streeter, R.G. Compton, Numerical simulation of potential step chronoamperometry at low concentrations of supporting electrolyte, J. Phys. Chem C 112 (35) (2008) 13716–13728.
[43] J.G. Limon-Petersen, I. Streeter, N.V. Rees, R.G. Compton, Quantitative voltammetry in weakly supported media: effects of the applied overpotential and supporting electrolyte concentration on the one electron oxidation of ferrocene in acetonitrile, J. Phys. Chem C 113 (1) (2009) 333–337.
[44] R. Armstrong, G. Horvai, Properties of PVC based membranes used in ion-selective electrodes, Electrochim. Acta 35 (1) (1990) 1–7.
[45] T.A. Nieman, G. Horvai, Neutral carrier potassium-selective electrodes with low resistances, Anal. Chim. Acta 170 (1985) 359–363.
[46] J.C. Scott, G.G. Malliaras, Charge injection and recombination at the metal–organic interface, Chem. Phys. Lett. 299 (2) (1999) 115–119.
[47] Y. Shen, M.W. Klein, D.B. Jacobs, J.C. Scott, G.G. Malliaras, Mobility-dependent charge injection into an organic semiconductor, Phys. Rev. Lett. 86 (17) (2001) 3867.